

Analyst

Accepted Manuscript



This is an *Accepted Manuscript*, which has been through the Royal Society of Chemistry peer review process and has been accepted for publication.

Accepted Manuscripts are published online shortly after acceptance, before technical editing, formatting and proof reading. Using this free service, authors can make their results available to the community, in citable form, before we publish the edited article. We will replace this *Accepted Manuscript* with the edited and formatted *Advance Article* as soon as it is available.

You can find more information about *Accepted Manuscripts* in the [Information for Authors](#).

Please note that technical editing may introduce minor changes to the text and/or graphics, which may alter content. The journal's standard [Terms & Conditions](#) and the [Ethical guidelines](#) still apply. In no event shall the Royal Society of Chemistry be held responsible for any errors or omissions in this *Accepted Manuscript* or any consequences arising from the use of any information it contains.

Biomolecular characterization of adrenal gland tumors by means of SR-FTIR

J. Dudala^{1*}, M. Bialas², A. Surowka¹, M. Bereza-Buziak³, A. Hubalewska-Dydejczyk³,
A. Budzynski⁴, M. Pedziwiatr⁴, M. Kolodziej⁵, K. Wehbe⁶, M. Lankosz¹

¹*AGH-University of Science and Technology, Faculty of Physics and Applied Computer Science,
Mickiewicza Av. 30, 30-059 Krakow, Poland,*

²*Chair and Department of Pathomorphology, Jagiellonian University, Medical College,
Grzegorzewska st. 16, 31-531 Krakow, Poland,*

³*Department of Endocrinology, Jagiellonian University, Medical College
Kopernika st. 17, 31-501 Krakow, Poland,*

⁴*2nd Department of General Surgery, Jagiellonian University, Medical College, Krakow, Poland,
⁵University Hospital, Krakow, Poland*

⁶*Diamond Light Source, Harwell Science and Innovation Campus, Didcot, Oxfordshire OX11 0DE, UK
e-mail: Joanna.Dudala@fis.agh.edu.pl

Abstract

The adrenal glands are small endocrine organs located on the bottom pole of each kidney. Anatomically they are composed of cortical and medullar part. Due to dysfunctional processes they can transform into the pathological lesions (in both cortex and medulla). The incidentally detected adrenal lesions have become an arising clinical problem nowadays. The crucial issue for accurate treatment strategy is the relevant diagnosis. Distinguishing between benign and malignant lesions is often difficult during the standard histological examination. Hence the alternative methods of differentiating are investigated. One of them is the Fourier transform infrared spectroscopy which allows analyzing the biomolecular composition of studied tissue. In this paper we present the very preliminary FTIR studies for defining the biomolecular pattern of three types of adrenal lesions: adenoma (AA) and adrenal cortical hyperplasia (ACH) – both derived from adrenal cortex as well as pheochromocytoma (PCC) – from medullar part of gland. All studied cases were classified as benign lesions. The general observations show that cortically derived tissues are rich in lipid and they are rather protein depleted while for medullar pheochromocytoma there is the opposite relation. Furthermore, the unequivocal differences were noticed within the “fingerprinting” range. In addition the subtle shifts of absorption bands position were observed between studied cases.

Keywords: adenoma, adrenal gland, FTIR, hyperplasia, neoplasm, pheochromocytoma, tumor

1. Introduction

The adrenal glands (suprarenal glands) are paired, small endocrine organs located in the retroperitoneum on the kidney surface. They consist of cortex and medulla which differ in their development and function. The adrenal cortex mainly plays a role in the regulation of water and electrolyte balance (via mineralocorticoids production) and modulates metabolism of proteins, carbohydrates and fat (via glucocorticoids production), while adrenal medulla is involved in reacting to stress and enabling rapid adaptation to changes in the environment. The adrenal medulla is composed of chromaffin cells which synthesize and secrete catecholamines (mainly epinephrine). Pathological lesions developing in adrenal glands differ in their nature depending on whether they are derived from cortical or medullar tissue. The most common cortical conditions include: different types of adrenal cortical hyperplasia (ACH); non-neoplastic lesion characterized by an increase in the number of cortical cells, usually forming one or many nodules (tumors) and causing increase in size of adrenal gland, as well as adrenal cortical adenoma (ACA) and adrenal cortical carcinoma (ACC), which are neoplastic lesions, benign and malignant respectively. The most common pathological condition connecting with adrenal medulla is pheochromocytoma (Ph, adrenal gland paraganglioma) [1].

Nowadays, when the image diagnostic methods develop rapidly, and they are easy accessible, the number of detected adrenal gland neoplastic lesions constantly increase. Nevertheless there is still the lack of the accurate criteria of surgical indication for adrenal incidentalomas [2]. The most important question, which should be considered, is whether the lesion tend to be malignant or it is rather a benign alteration. The proper diagnosis is crucial for the further medical treatment and its consequences for the patients. It is generally agreed that the absolute indication for adrenalectomy is the tumor size (generally of the diameter > 4 cm) and increased hormonal activity. However in some cases the lesions which do not exceed the determined size and do not reveal the hormone overproduction occurred to be malignant in the future. Admittedly there are some clinical classification methods which help to differentiate between malignant and benign lesion but there is still lack of a biomarker which could indicates the cancerous progression itself [3-6].

In the presented paper we propose applying the Fourier transform IR (FTIR) spectroscopy. This method allows for both qualitative and quantitative analysis of the basic components of biological tissues. Routinely a histopathological examination of biopsy sample or intraoperative material is used for diagnosis but the literature review revealed that FTIR microspectroscopy is used more and more frequently as a complementary diagnostic method [7-10]. Its ability of detecting the subtle chemical changes in human tissue samples allow for considering this method as molecular histopathology.

2. Experimental

Sample preparation

In our study the archival tissue samples from different types of adrenal gland lesions were used. They were obtained from the Pathomorphology Department, Medical College, Jagiellonian University in Krakow, Poland. The study was approved by the Jagiellonian University Bioethical Committee (KBET/113/B/2014). The specimens were taken intraoperatively from patients with adenoma and hyperplasia - both derived from cortical part of adrenal gland and pheochromocytoma derived from adrenal medulla. From each sample, two sections of 6 μm thick were cut in a cryo-microtome during the sample preparation. One slice was placed on a basic slide for histological purpose and the second one - for FTIR measurements was mounted on silver coated sample supports (Low-e MirrIR, Kevley Technologies) and freeze-dried at the temperature $-80\text{ }^{\circ}\text{C}$. There were two samples of each lesion type (adenoma, hyperplasia and pheochromocytoma) used for biomolecular composition study. All investigated samples were classified in the Pathomorphology Department of Medical College, Jagiellonian University as benign lesions.

FTIR data collection

The measurements were carried out at the MIRIAM beamline at Diamond Light Source, UK, using Bruker Vertex 80V Vacuum-FTIR interferometer coupled with the Bruker Hyperion 3000 microscope (fully automated microscope with a liquid nitrogen cooled MCT detector). Spectral images were collected using Synchrotron Radiation (SR) source in transfection-mode in the range of $4000 \div 400\text{ cm}^{-1}$ at 4 cm^{-1} spectral resolution using the $36\times$ objective. The beam was defined by aperture size of $6\text{ }\mu\text{m} \times 6\text{ }\mu\text{m}$, the step size was set to $3\text{ }\mu\text{m}$; 128 and 256 scans per spectrum were accumulated respectively for tissue sample and background position.

FTIR data processing and analysis

Data processing was performed using the OPUS 7.0 software (Bruker Optics, Ettlingen-Germany). Two types of analysis were applied – one for a general biomolecular comparison of studied adrenal lesions and the second – for classifying the obtained spectra.

For the first reason the following procedure was applied: 50 spectra of good quality were chosen for the analysis from each studied sample (two samples per each case). From each chosen spectra the range of $3040 \div 950\text{ cm}^{-1}$ was separated for the further analysis. Then all selected spectra, of one lesion type, were averaged hence we obtain one averaged spectrum for a proper adrenal gland lesion case. Subsequently it was baseline corrected, using the concave rubber band algorithm (10 iterations and 64 points), and then vector normalization was applied. To determine the main absorption bands the minimal values of the second-derivative spectra were used.

In order to classify the studied adrenal lesions the hierarchical cluster analysis (HCA) was used. This is an unsupervised classification method which allows grouping analyzed spectra into clusters depending on their “similarity”. The clustering is based on the comparison of spectral distances between analyzed spectra, the higher value of spectral distance means higher difference between compared spectra. In the presented study the spectral distance was calculated with standard method using the Euclidian distance and Ward’s criterion. The calculations were done for the second derivative and vector normalized spectra with 9 smoothing points.

3. Results and discussion

From biological point of view within mid-IR range there are some spectral regions particularly interesting hence they were used for the further analysis. The first one covers the absorption bands between 3040 cm^{-1} and 2780 cm^{-1} and it is attributed to the lipid content. The next one, of rather mixed biological character, extends from about 1770 cm^{-1} up to 950 cm^{-1} and relates to lipids, proteins, nucleic acids, phosphates and carbohydrates [11, 12]. Within this spectral interval, we were able to find four clearly visible subregions, which could be used for a rapid comparison between studied samples; they are as follow: $\sim 1770\div 1480\text{ cm}^{-1}$, $\sim 1480\div 1350\text{ cm}^{-1}$, $\sim 1350\div 1150\text{ cm}^{-1}$ and $\sim 1150\div 990\text{ cm}^{-1}$.

From the obtained results the most visible differences between studied tissue samples are related to the lipid and protein amount. It is seen that the lipid content in adenoma and hyperplasia are higher than in pheochromocytoma samples (cf. Fig.1A). On the other hand the absorbance within the region between 1700 cm^{-1} and 1480 cm^{-1} , related mainly to the protein, is higher for the pheochromocytoma cases (cf. Fig. 2A). The observed biochemical composition reflects a physiological role of a particular section of adrenal gland tissue. The cortical part of adrenal gland produces hormones being the derivatives of cholesterol hence in adenoma and hyperplasia the level of lipids are high; a medullar part of adrenal gland secretes hormones being the derivatives of amino acids hence the protein level in pheochromocytoma is higher.

To determine the main absorption bands the second-derivative spectra, averaged for each studied case, were used. In the lipid region ($3040\div 2780\text{ cm}^{-1}$) there are five main bands; $\sim 3011\text{ cm}^{-1}$, $\sim 2959\text{ cm}^{-1}$, $\sim 2921\text{ cm}^{-1}$, $\sim 2873\text{ cm}^{-1}$, $\sim 2852\text{ cm}^{-1}$ which relates respectively to the stretching vibrations of $\nu(\text{=CH})$, $\nu_{\text{as}}(\text{CH}_3)$, $\nu_{\text{as}}(\text{CH}_2)$, $\nu(\text{CH}_3)$, $\nu(\text{CH}_2)$. The olefinic band at around $\sim 3011\text{ cm}^{-1}$ is clearly seen in adenoma and hyperplasia cases while in pheochromocytoma it is hardly visible. Comparing the position of the asymmetric stretching band related to $\nu_{\text{as}}(\text{CH}_3)$ it seems that in case of adenoma and hyperplasia the band of $\nu_{\text{as}}(\text{CH}_3)$ splits up in two peaks located at $\sim 2963\text{ cm}^{-1}$ and $\sim 2954\text{ cm}^{-1}$ while in pheochromocytoma it is placed at $\sim 2959\text{ cm}^{-1}$. Regarding the band related to the $\nu_{\text{as}}(\text{CH}_2)$ in adenoma and hyperplasia there is a tendency for moving up the position of that peak to the higher wavenumber at around 2927 cm^{-1} while for pheochromocytoma it is located at $\sim 2922\text{ cm}^{-1}$. The remaining symmetric stretching bands for all studied samples are approximately at the same position $\sim 2873\text{ cm}^{-1}$ and $\sim 2852\text{ cm}^{-1}$ for $\nu(\text{CH}_3)$ and $\nu(\text{CH}_2)$ respectively. The second derivative analysis allowed finding in pheochromocytoma another, very subtle, absorption bands at $\sim 2900\text{ cm}^{-1}$ which seems to be cloven in cortical derived samples for two small bands at around 2902 cm^{-1} and 2888 cm^{-1} .

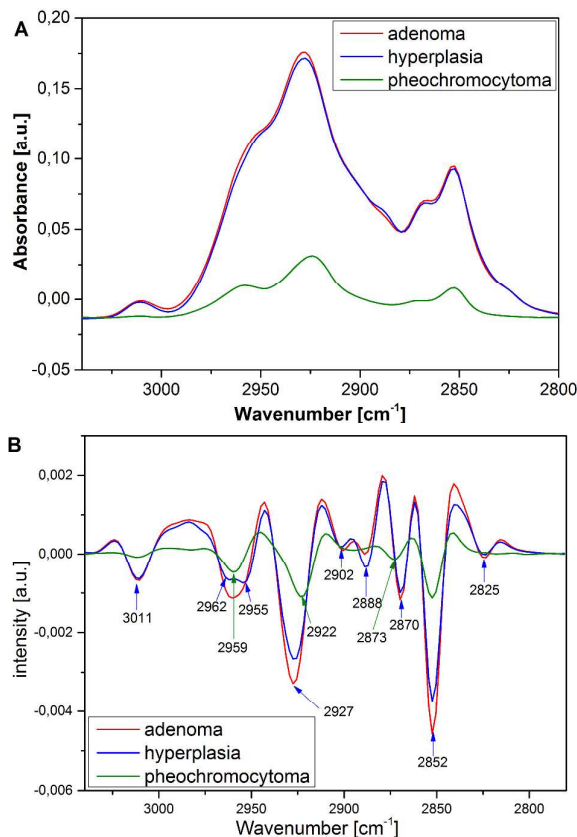


Fig. 1. The averaged spectra for adenoma, hyperplasia and pheochromocytoma within the range of 3040÷2780 cm⁻¹, A) the baseline corrected and vector normalized absorption spectra, B) the second-derivative spectra with marked minimum values which point the main absorption bands.

In the similar way the absorption bands were found within the region between 1770 cm⁻¹ and 950 cm⁻¹. Within this rather wide region four spectral subregions can be distinguished as follows: 1780÷1480 cm⁻¹, 1480÷1350 cm⁻¹, 1350÷1150 cm⁻¹ and 1150÷950 cm⁻¹. The reason of dividing in such a manner was the possibility of quick comparison of spectral pattern between the studied adrenal gland lesions. In the first spectral region the absorption band, exhibiting the highest intensity especially for cortically derived tissue, was found to be centered at ~1736 cm⁻¹ due to the C-O stretching vibrations of esters; the next two absorption masses were set as follow: at ~1655 cm⁻¹ (amide I), which arises from the $\nu(\text{C}=\text{O})$ stretching vibrations of the amide groups of the protein backbone, while the absorption band centered at ~1545 cm⁻¹ (amide II) arises from the $\delta(\text{N-H})$ bending vibrations. It is observed that the position of the acid ester band in pheochromocytoma is shifted to the higher wavenumber (~1741 cm⁻¹) while in adenoma and hyperplasia this peak is located at ~1736 cm⁻¹. In all studied samples it was also noticed the lipid ester at around 1710 cm⁻¹ while in pheochromocytoma the band at ~1725 cm⁻¹ was additionally detected. Within the range of amide I there were found four consecutive absorption bands: ~1694 cm⁻¹, 1682 cm⁻¹, 1655 cm⁻¹, 1638 cm⁻¹; they relates respectively to the antiparallel and parallel β -sheet structure, α -helix and triple helix of collagen. In the massif of amide II the following bands were discovered in all studied cases: amine band $\delta(\text{NH}_2)$ at ~1596 cm⁻¹, amide II at ~1571 cm⁻¹, amide III at ~1548 cm⁻¹ and tyrosine rings at ~1513 cm⁻¹. Any observed shifts within the region of amide I and amide II could arise from the alteration in the secondary structure of intracellular proteins which can be attributed to the pathological molecular changes [8,12].

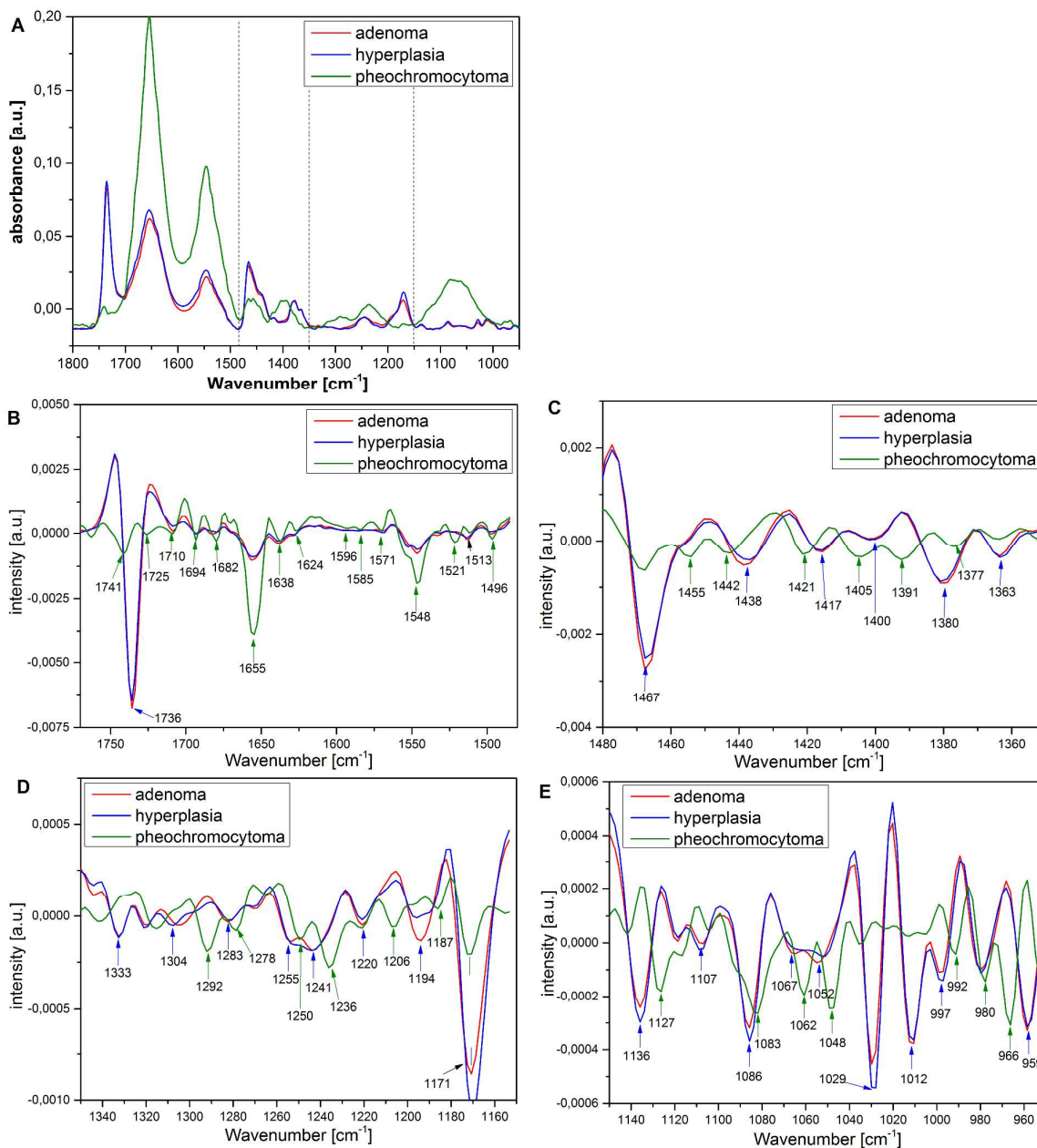


Fig. 2. The averaged spectra for adenoma, hyperplasia and pheochromocytoma within the range of 1770÷950 cm⁻¹, the dashed lines separate four distinguished spectral region A) the baseline corrected and vector normalized absorption spectra; the second-derivative spectra with marked minimum values which point the main absorption bands within the following regions: B) 1770÷1480 cm⁻¹, C) 1480÷1350 cm⁻¹, D) 1350÷1150 cm⁻¹, E) 1150÷950cm⁻¹.

The spectral range of wave numbers between 1500 cm⁻¹ and 600 cm⁻¹ is commonly regarded as the “fingerprinting region”. It brings a huge amount of information about the biocomposition of studied samples, emerged from the vibrations related to the proteins, lipids, nucleic acids, phosphates and carbohydrates. The problem of analysis within the “fingerprinting region” arises from overlapping bands, which makes it difficult to adjust properly the particular band with the proper functional group as well as to evaluate semi-quantitatively the content of individual biomolecules [11]. For the purpose of the presented work the “fingerprinting region” was divided for intervals, as it was said before, which help to compare visually the studied tissue samples. Within the spectral interval 1480÷1350 cm⁻¹ there is a considerable difference between cortical and medullar derived tissue samples. This spectral section is attributed mainly to the lipids and the main absorption bands at around ~1466 cm⁻¹ and ~1380 cm⁻¹ relate respectively to $\delta_{\text{asym}}(\text{CH}_3)$ asymmetric and $\delta(\text{CH}_3)$ symmetric bending vibrations. In pheochromocytoma cases these two peaks are relatively small comparing to the adenoma and hyperplasia samples in which these are very intense massifs. Besides it seems that in adenoma and hyperplasia the absorption band related to the $\delta(\text{CH}_3)$ symmetric bending vibrations is located at ~1380 cm⁻¹ while in pheochromocytoma it moves for the higher wavenumbers at

around 1390 cm^{-1} .

The absorption bands present within the next discussed spectral interval ($\sim 1350\div 1150\text{ cm}^{-1}$) are mainly attributed to the massif of amide III ($\sim 1330\div 1230\text{ cm}^{-1}$) but there is also ascribed the band related to the asymmetric stretching vibrations of phosphates $\nu_{\text{as}}(\text{PO}_2)$ at $\sim 1245\div 1230\text{ cm}^{-1}$. Additionally there is an absorption band at $\sim 1170\text{ cm}^{-1}$ which arises from the ester asymmetric stretching vibration $\nu_{\text{as}}(\text{C-O})$. The absorption intensity of this vibration is the most visible difference between analyzed spectra; for medullar pheochromocytoma it is rather small comparing to the cortical derived samples for which it is the peak of significant intensity.

In the region of the wavenumbers below $\sim 1150\text{ cm}^{-1}$ the absorption bands are mainly attributed to the nucleic acids but also to the carbohydrates and phosphorylated protein. As far as pheochromocytoma is considered it is seen very intense massif spreads over the range $\sim 1150\div 1000\text{ cm}^{-1}$ while for cortical adenoma and hyperplasia there are many separate absorption bands of low intensity. The most intense absorption bands for cortically derived samples within this region are located at around $\sim 1136\text{ cm}^{-1}$, $\sim 1086\text{ cm}^{-1}$ and $\sim 1029\text{ cm}^{-1}$ while for medullar tissue they seem to be shifted and located at $\sim 1127\text{ cm}^{-1}$, 1083 cm^{-1} , $\sim 1062\text{ cm}^{-1}$ and $\sim 1048\text{ cm}^{-1}$. The mutual dependence of the $\sim 1086\text{ cm}^{-1}$ and $\sim 1029\text{ cm}^{-1}$ bands, respectively attributed to the phosphate and glycogen ratio, is treated as an indirect indicator of cellular metabolic turnover and is believed to be a potential cancer biomarker [8]. As this “fingerprinting region” is strictly related to the DNA and RNA composition it is important to find out if there is any relation between the level of such biomolecules and the Ki-67/MIB1 labeling index. This is the cellular marker for the proliferation processes. Its value increases in case of cancerous progression [13, 14]. In future we are planning to find out if there is any relation between the proliferation index and the nucleic acid contents in benign and malignant lesions.

The obtained results allow establishing a specific biomolecular pattern for neoplastic adenoma and pheochromocytoma and non-neoplastic hyperplasia. Characteristic parameters differentiating the studied cases are the intensity of particular band as well as subtle shifts of bands’ positions. In studied cases many observed shifts are at the level which is comparable with the spectral resolution (4 cm^{-1}) but there is a clear tendency for that.

For the classification of studied tissue samples the hierarchical cluster analysis was used. This unsupervised method allows to group spectra into clusters according to their “similarity”. As an input component we used the second derivative, vector normalized spectra with 9 smoothing points. There were 300 spectra analyzed altogether (100 per each studied case – 50 spectra for each sample) and a standard method, based on Euclidean distance, was used for classification. As input parameters the earlier discussed spectral ranges or combinations of ranges were used to find out, which wavenumbers’ range groups the studied cases in the most appropriate way. Figure 3 presents dendrograms obtained as a result of HCA for different spectral ranges taken as a clustering parameter. Regardless of clustering spectral parameter the presented results revealed that the studied spectra are clustered in two groups. With 100% accuracy one of them gathers both adenoma and hyperplasia samples while the pheochromocytoma cases are attributed to the separated group.

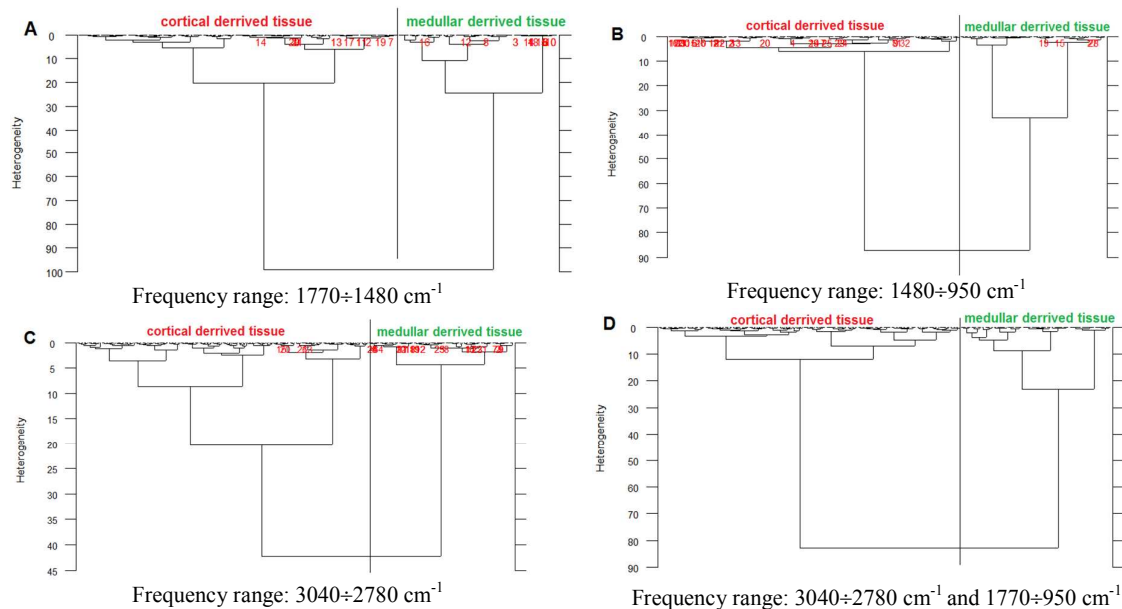


Fig. 3. Cluster analysis of second-derivative spectra using the spectral range: A) $1770\div 1480\text{ cm}^{-1}$, B) $1480\div 950\text{ cm}^{-1}$, C) $3040\div 2780\text{ cm}^{-1}$, D) $3040\div 2780\text{ cm}^{-1}$ and $1770\div 950\text{ cm}^{-1}$

This is not a surprising observation because both - adenoma and hyperplasia derive from the same anatomical part of adrenal gland so that they are biochemically similar and different from pheochromocytoma cases.

From the comparison of the obtained results it seems that the best separation parameter differentiating the two groups is the protein region of $1770\div 1480\text{ cm}^{-1}$. The heterogeneity between separated groups is at the level of 95%. Furthermore this spectral region does not cause the inner group heterogeneity as it is at about 18% for cortical tissue and 23% for medullar

1
2
3 lesions (cf. Fig.3A). We obtained similar results for the “fingerprinting” region of 1480±950 cm⁻¹ as clustering parameter. In
4 this case the heterogeneity between separated cortical and medullar groups is at the level of 90%. This spectral range is
5 resembled for adenoma and hyperplasia (about 5% inner group heterogeneity) but pheochromocytoma samples distinguishing
6 for two sup-groups which differ at the level of 30% (cf. Fig. 3B). The weakest clustering parameter is the lipid region
7 (3040±2780 cm⁻¹). In this case the heterogeneity between two groups is about 43% (cf. Fig. 3C). We also tried to mix the
8 spectral ranges as a clustering parameter and the results were comparable with those obtained for the protein range parameter,
9 however slightly worse (cf. Fig. 3D).

10 Conclusions

11 The presented results account for the first step of biochemical studies of adrenal gland tumors. The outcomes have a
12 preliminary character but enable the comparison of three types of adrenal gland pathological lesions – cortically derived
13 adenoma and hyperplasia as well as pheochromocytoma originating from medullar part. All studied tissue samples were
14 classified by pathologist as not malignant, benign lesions. In the next step of researches we are planning to find out the
15 biocomposition of adrenal carcinoma which is very aggressive and bad promising malignant lesion. The various processes
16 lead to the tumor progression; the affected tissue can be modified anatomically and biochemically. For example growing
17 tumor mass needs more oxygen and glucose comparing to the healthy tissue. This results in angiogenesis and changes of
18 biochemical composition of tumor tissue comparing to corresponding benign or non-neoplastic tissue [15, 16]. The efforts
19 have to be made to find a spectral biomarker of malignancy phenotype. It might include the biomolecule contents as well as
20 the shifts of the particular absorption bands. Having such a biomarker/s it might be possible to extend currently used
21 diagnostic method. Probably the core needle biopsy of the adrenal glands would be possible as it is believed that spectral
22 pattern of the biopsy material could help to predict the malignancy progression within a studied case and to modify the
23 treatment method.

24 Acknowledgements

25 This work was supported by the Polish Ministry of Science and Higher Education and its grants for Scientific Research. This
26 work was carried out with the support of the Diamond Light Source, the UK national synchrotron (projects: SM7635,
27 SM8780).

28 References

- 29 1. Lack, E.E. *Tumors of the Adrenal Glands and Extraadrenal Paraganglia, AFIP Atlas of Tumor Pathology*, series
30 4; ARP Press Silver Spring: Maryland, 2007, pp. 1-35, 57-124, 241-274.
- 31 2. T. Nishikawa, J. Saito and M. Omura, *Biomed Pharmacother*, 2002, **56**, 145–148.
- 32 3. R. H. Grogan, E. Mitmaker, M. R. Vriens, A. Harari, J. E. Gosnell, W. T. Shen, O. H. Clark and Q-Y. Duh,
33 *Surgery*, 2010, **148**, 392-397.
- 34 4. G.G. Fernandez-Ranvier, J. Weng, R.F. Yeh, E. Khanafshar, I. Suh, C. Baker et. al, *Arch Surg*, 2008, **143**, 841-846.
- 35 5. C. Proye, M. Jafari Manjili, F. Combemale, F. Pattou, O. Ernst, B. Carnaille and J.L Wemeau, *Arch Surg*, 1998,
36 **383**, 330-333.
- 37 6. L. Barzon and M. Boscaro, *The Journal of Urology*, 2000, **163**, 398-407.
- 38 7. M. Walsh, M. German, M. Singh, H. Pollock, A. Hammiche, M. Kyrigiou, H. Stringfellow, E. Paraskevidis, P.
39 Martin-Hirsch and F. Martin, *Cancer Letters*, 2007, **246**, 1-11.
- 40 8. M. Walsh, M. Singh, H. Pollock, L. Cooper, M. German, H. Stringfellow, N. Fullwood, E. Paraskevidis, P.
41 Martin-Hirsch and F. Martin, *Biochemical and Biophysical Research Communications*, 2007, **352**, 213-219.
- 42 9. K. Das, C. Kendall, I. Martin, C. Fowler, J. Christie-Brown and N. Stone, *Journal of Photochemistry and*
43 *Photobiology B: Biology*, 2008, **92**, 160-164.
- 44 10. H. Fabian, P. Lasch, M. Boese and W. Haensch, *Journal of Molecular Structure*, 2003, **661-662**, 411-417.
- 45 11. G. Bellisola and C. Sorio, *Am J Cancer Res*, 2012, **2(1)**, 1-21.
- 46 12. C. Petibois and G. Deleris, *Trends in Biotechnology*, 2006, **24(10)**, 455-462.
- 47 13. M. Terzolo, A. Boccuzzi, S. Bovio, S. Cappia, P. De Giuli, A. Ali, P. Paccotti, F. Porpiglia, D. Fontana and A.
48 Angeli, *Urology*, 2001, **57**, 176-182.
- 49 14. M.P. Vargas, H.I. Vargas, D.E. Kleiner and M.J. Merino, *Am J Surg Pathol*, 1997, **21**, 556-562.
- 50 15. P. Carmeliet and R.K. Jain, *Nature*, 2004, **407**, 249-257.
- 51 16. S. Sharma, M.C. Sharma and C. Sarkar, *Histopathology*, 2005, **46**, 481-489.
- 52
- 53
- 54
- 55
- 56
- 57
- 58
- 59
- 60